Q. J. R. Meteorol. Soc. (1994), **120**, pp. 211–226 551.581.1:551.509.313.32:551.513.1

The impact of changing the horizontal diffusion scheme on the northern winter climatology of a general circulation model

By DAVID B. STEPHENSON*
University of Reading, UK

(Received 2 August 1993; revised 3 February 1994)

SUMMARY

A general circulation model was used in perpetual January mode, to study the wintertime climatological sensitivity to changes in the horizontal hyper-Laplacian diffusion scheme at both spectral T21 and T42 horizontal resolutions.

Analysis of the global energy cycle revealed a large impact especially on the conversion of eddy to zonal kinetic energy. Less diffusion resulted in less zonal available potential energy, weaker baroclinic conversions and caused the barotropic conversion of eddy to zonal kinetic energy to become significantly weaker. It was found that by weakening the diffusion in the T21 model, the eddy kinetic energy increased and became more realistic yet at the same time the conversion of eddy to zonal kinetic energy decreased and became less realistic.

Weakening the horizontal diffusion caused a northern hemisphere tropospheric response similar to that obtained by increasing the upper-level orographic gravity wave drag in the model. The zonal-mean zonal winds weakened poleward of the subtropical jets, the Ferrel cells weakened and the troposphere warmed up at high latitudes. The weakening of the zonal wind and the Ferrel cells was associated with a weakening of the upper-level convergence of the poleward eddy momentum flux and the wave-mean flow interaction was demonstrated using Eliassen–Palm diagnostics. A substantial part of the change in the poleward eddy momentum flux was due to large changes in the poleward momentum flux of the transient eddies in the mid-latitude stormtracks and changes in their horizontal phase tilt. A large northern hemisphere stationary-wave change appeared in these regions and had a similar structure in the Atlantic sector to that seen when strengthening upper-level gravity wave drag.

1. INTRODUCTION

Present-day atmospheric general circulation models (GCMs) have grid spacings of the order of a few hundred kilometres and are incapable of describing horizontal mixing of air masses on spatial scales smaller than this. As vortex filaments become stretched out, curl up and break in the atmosphere, potential enstrophy cascades from the large synoptic to the smaller scales. In the absence of a horizontal diffusion parametrization to account for mixing on the unresolved scales, potential enstrophy is forced to accumulate at the smallest scales in the model. Such an accumulation, known as spectral blocking, results in a deviation from the observed k^{-3} energy spectra and is visible as excessive small-scale noise in such quantities as potential vorticity. To avoid this, it is necessary to include horizontal diffusion schemes in GCMs which imitate sub-grid scale mixing by removing potential enstrophy at the small scales. In the absence of a unique closure scheme, an infinity of possible heuristic schemes exist for parametrizing the unresolved horizontal mixing. It is hoped that as the resolution of models is increased, it will be possible to tune the diffusion schemes to give large-scale results in agreement with the observations. Because of the non-linear interactions between all spatial scales in the atmosphere, it is not clear that all schemes will converge as this limit is taken.

The most commonly used schemes are of the hyper-Laplacian form where the time-tendency of the vorticity, divergence, temperature and humidity fields is given by:

$$\frac{\partial \chi}{\partial t} = -(-1)^q K \nabla^{2q} \chi \tag{1}$$

where χ is the field on either pressure or sigma surfaces. The case of $q = 1$ was used by Bourke (1974) and is the physically meaningful Fickian diffusion process. Whether or

* Corresponding address: Météo-France, 42 ave. G. Coriolis, 31057 Toulouse Cedex, France.

not Fickian diffusion adequately describes nonlinear mixing processes in the atmosphere is a debatable question (Pierrehumbert 1991). It was found that in order to damp the small scales sufficiently with such a scheme, such large values of κ were necessary that the large scales were also significantly damped; the scheme was not sufficiently scale-selective. Because of the computational speed of applying the Laplacian operator in spectral models, hyper-diffusion schemes with $q > 1$ have been widely used and are the focus of the study in this paper. A linear growth rate study of baroclinic waves was performed with a 5-level T42 GCM by MacVean (1983) who showed that the ubiquitous ∇^4 schemes ($q = 2$) affected significantly the linear stability of almost all wavenumbers and it was recommended that $q > 2$ schemes should be used to obtain good representations of baroclinic waves. Another form of linear scale-selective scheme was introduced by Boer *et al.* (1984) and in spectral space involves using a two piece piecewise-function of total wavenumber, n, rather than using the function $(n(n + 1))^q$ corresponding to the more traditional diffusion in Eq. (1). The small-n piece, corresponding to the large spatial scales, is invariably set to zero whilst the high-n piece is set to some power of n. This form has the advantage of being scale-selective but has no easy interpretation in terms of continuum derivative operators. More esoteric non-linear schemes have been developed such as that of Smagorinsky (1963) and that of Sadourny and Basdevant (1985). The Anticipated Potential Vorticity Method (APVM) of Sadourny and Basdevant (1985) has the virtue of destroying potential enstrophy on the smallest scales yet still conserving kinetic energy and it may be more appropriate for describing the sub-grid scale mixing processes. Unfortunately, the scheme is defined on isentropic surfaces which makes it difficult to implement in tropospheric GCMs where the isentropic surfaces can intersect the ground.

Although the choice of scheme is seemingly so arbitrary and the possible impact on the model results is large, relatively few horizontal diffusion studies have been performed with realistic GCMs. The effect of horizontal diffusion schemes on the behaviour of the mid-latitude baroclinic waves, especially during the barotropic decay phase of their lifecycles, may be crucial in accurately reproducing the general circulation. Klinker and Sardesmukh (1992), in a study of the systematic errors in the European Centre for Medium-range Weather Forecasts (ECMWF) forecast model momentum budget, suggest that there is an error in the poleward momentum flux arising from the misrepresentation of the potential enstrophy cascade in stormtrack regions that lie slightly poleward of the jets and imply that the description of horizontal mixing may be to blame. The fact that mid-latitude storms are sensitive to the choice of diffusion scheme was demonstrated by MacVean (1983) in baroclinic lifecycle studies where a large impact was found on the conversion of eddy kinetic energy to zonal kinetic energy. Furthermore, Eliasen and Laursen (1990) showed that the poleward momentum fluxes in a two-layer GCM were sensitive to the choice of horizontal diffusion scheme and this was confirmed by Held and Phillips (1993) in their experiments with the 9-level R15 Geophysical Fluid Dynamics Laboratory GCM. Previous attempts to tune horizontal diffusion schemes have attempted to adjust the parameters to give the observed k^{-3} energy spectrum (Laursen and Eliasen 1989). This approach will not be followed in this paper for two reasons. Firstly, in order to give the best simulation of the large-scale circulation, it is not obvious that a finite truncation model should be forced to have the same spectral slope as the continuum; an accumulation of energy at the small scales may be necessary to account for the missing energy in the unresolved scales. Secondly, because the horizontal diffusion schemes are not perfect closure schemes, having a good energy spectrum is no guarantee that other quantities such as momentum fluxes will be well simulated; tuning to get a good energy spectrum is only one of many possible ways to tune the scheme. Because of the crucial

role played by mid-latitude transients in the general circulation of the atmosphere, in their role in the teleconnections from El Niño-Southern Oscillation events (Held *et al.* 1989) and in doubled CO_2 climate change experiments (Stephenson and Held 1993), it is important to further understand their sensitivity to changes in the horizontal diffusion scheme.

This paper is an attempt to understand the magnitude and nature of the impact of changing the parameters in a horizontal diffusion scheme on the wintertime climatology of a realistic GCM. Because of the wide use of hyper-Laplacian schemes and because of their simplicity compared to nonlinear schemes it was decided to examine the model behaviour in the context of such schemes with the hope that future studies will be performed with the other classes of possible schemes. Both low and high horizontal resolution versions of the model were used in order to compare the response and assess its stability with respect to model resolution. The question of whether or not a low resolution model can be tuned to give the more realistic climatology obtained with high resolution models, without having the well known defects of too little eddy kinetic energy and too feeble eddy momentum fluxes, is addressed by means of an energy budget analysis. A description of the model and experiments is given in section 2 followed by a presentation of the results in section 3 and finally a discussion is presented in section 4.

2. Experimental method

(*a*) *The model*

The GCM used in these studies is the UK Universities' Global Atmospheric Modelling Programme (UGAMP) model which was derived from the 1987 cycle 27 ECMWF spectral forecast model described by Tiedtke *et al.* (1988) and Palmer *et al.* (1990). The radiation parametrization of Morcrette (1990) is used and deep convection is parametrized by the Kuo scheme as described in Tiedtke *et al.* (1988). The model has a diurnal cycle and has January mean sea surface temperatures prescribed from the climatology of Alexander and Mobley (1976). It has been found that a truncation of T42 and 19 vertical levels gives results in reasonable agreement with northern hemisphere wintertime observations whereas at lower resolutions such as T21 the transient features in the northern hemisphere stormtracks are poorly simulated with too little eddy kinetic energy and too weak poleward eddy momentum fluxes in mid-latitudes. For a description of the model's performance at simulating the analysed wintertime climatology refer to Boer *et al.* (1991, 1992). In this paper, both spectral horizontal truncations of T21 and T42 having 19 vertical levels extending up to around 10 mb are used to study the sensitivity to changes in the horizontal diffusion scheme.

(*b*) *The horizontal diffusion scheme*

As with the ECMWF forecast model, the UGAMP GCM uses a hyper-Laplacian diffusion scheme to parametrize the horizontal sub-grid scale mixing processes. A time-tendency term of the form given in Eq. (1) is included in the model vorticity, divergence, temperature, and humidity equations. This paper examines the model behaviour, at both T21 and T42 resolutions, to changes in the parameters (κ, q). Following MacVean (1983), it is more convenient to refer to the damping strength, κ, by the time-scale, τ, of the damping at the model's smallest horizontal scale. The damping time is given by the expression $\tau = L_{\min}^{2q}/\kappa$, with the minimum length scale resolved by the model at triangular resolution TN defined as $L_{\min} = a/\sqrt{N(N+1)}$, where a is the radius of the earth. As an example, the ECMWF forecast model at T42 resolution has a minimum length scale,

$L_{\min}$, of 150 km and uses values of $q = 2$ and $\kappa = 2 \times 10^{15}\ \mathrm{m^4\ s^{-1}}$ corresponding to a smallest-scale damping time, τ, of 70 hours (about 3 days); this will be referred to as either $70\,\mathrm{h}\,\nabla^4$ or $3\,\mathrm{d}\,\nabla^4$ damping in what follows*. MacVean (1983) found a strong sensitivity of baroclinic wave growth rates for $q \leqslant 2$ at T42 resolution and empirically found that $\tau \leqslant 1$ day was necessary to obtain spatially smooth solutions. Whilst typical time-scales for sharpening of fronts is about 6 hours, it is far from clear what value of τ should be used as is evidenced from values ranging from hours to weeks used in the different GCMs worldwide. Nor is it clear that the scheme is ideally suited to describing mid-latitude synoptic features in all their complexity especially such features as cut-off low formation, vortex roll-up, and filament formation.

(c) *The simulations*

Because of the cheaper computational cost, the T21 model was used to investigate (τ, q) space by taking nine points covering all possible combinations of $q = 3$, 4, 5 and $\tau = 4$ hours, 1 day and 6 days. The diffusion is weaker for both the case of larger τ and for the case of larger q where the diffusion has less effect on the larger-scale waves.

The case of no diffusion was not performed because of the following reason. As with taking the Reynolds number to infinity in a numerical turbulence simulation, for any fixed resolution there is a maximum achievable Reynolds number constrained by the fact that the Kolmogorov scale† must be resolvable on the grid. As with turbulence, the limit, as the diffusion strength is reduced to zero, is not the same as the case of zero diffusion and for climate models it is the limiting process and not the inviscid case which is of interest. Hence the effective simulation of high Reynolds number flow depends on carefully tuning the diffusion to zero as the model resolution is increased.

At T42, only two points in (τ, q) space were studied corresponding to the case of strong and weak diffusion. For the strong diffusion case, the value of $4\,\mathrm{h}\,\nabla^6$ was used corresponding to values currently used in the UGAMP GCM and at ECMWF. For the weak diffusion case, the value of $1\,\mathrm{d}\,\nabla^{10}$ was used. As is to be expected, the weak diffusion case gives potential vorticity maps looking noisier than the strong diffusion case yet both values of τ are within the range used by current GCMs and are not unreasonable values to use for the scheme. By looking at the difference of results between two possible reasonable choices, it will be demonstrated that tuning the horizontal diffusion scheme in a model is a necessary and difficult exercise.

All the runs were performed in perpetual January mode with fixed insolation and sea surface temperatures appropriate to January. The T21 model was allowed 45 days to spin-up from 15 January 1987 conditions and then time-averages were made from the outputs taken every 18 hours for the next 180 days. The T42 model was allowed 60 days to spin-up from 15 January 1987 initial conditions and then time-averages were made from the results taken every 18 hours for the next 240 days. The spin-up period was chosen by regarding the approach to equilibrium of global mean quantities such as kinetic energy in previous simulations with the model. Although the period of these climate runs is rather short, the similar features seen in the T42 and T21 models, the underlying dynamical explanation and the strength of the response give confidence that the response is that due to changes in the diffusion scheme and not solely natural variability of the model atmosphere. Both the T21 and T42 responses for the $1\,\mathrm{d}\,\nabla^{10}$ minus the $4\,\mathrm{h}\,\nabla^6$ cases, i.e. the weak minus strong diffusion response, will be shown in the following section in order to illustrate the common features and the large response even at T42.

* This is used for all except the divergence equation which uses a larger value of $\kappa = 5 \times 10^{15}\ \mathrm{m^4\ s^{-1}}$ to damp small-scale convective noise.

† The scale at which advection and diffusion become comparable.

3. Results

(a) *Global energetics*

The aim of this section is to examine the response of the global energy cycle to changes in the horizontal diffusion scheme. The conversion of energy between the different components of the global energy budget gives an encompassing view of the general circulation and shows clearly the baroclinic and barotropic conversions associated with the growth and decay of mid-latitude disturbances. Rather than use the partitioning proposed by Lorenz (1955), it was decided to use the definition for available potential energy (APE) proposed by Pearce (1978) which facilitates an easier interpretation of APE in terms of the spatial distribution of the temperature variance and the associated heat sources and sinks.

Figure 1 shows a diagram of the global energy cycle obtained from a four times daily T106 ECMWF analysis of the 1990/91 DJF winter after interpolation onto a 19-level T42 model grid. Differential diabatic heating rates in the atmosphere give rise to spatially distributed heat sources and sinks, which cause energy to be supplied to the static stability (AS), the zonal (AZ) and the eddy (AE)* components of the available potential energy. Baroclinic instability then causes the available potential energy to be converted into eddy kinetic energy (KE) associated with baroclinic waves. Some of this energy is dissipated to friction whilst the remainder is converted to zonal kinetic energy (KZ) by the mature baroclinic waves reinforcing the zonal flow by the barotropic convergence of poleward momentum flux. The dashed lines in Fig. 1 denote minor conversions with much smaller conversion rates than the major conversions described above. It is a property of the Pearce definition that the sum of the conversion rates from AE and AS to KE in the Pearce scheme equals the conversion rate of APE to eddy kinetic energy in the Lorenz

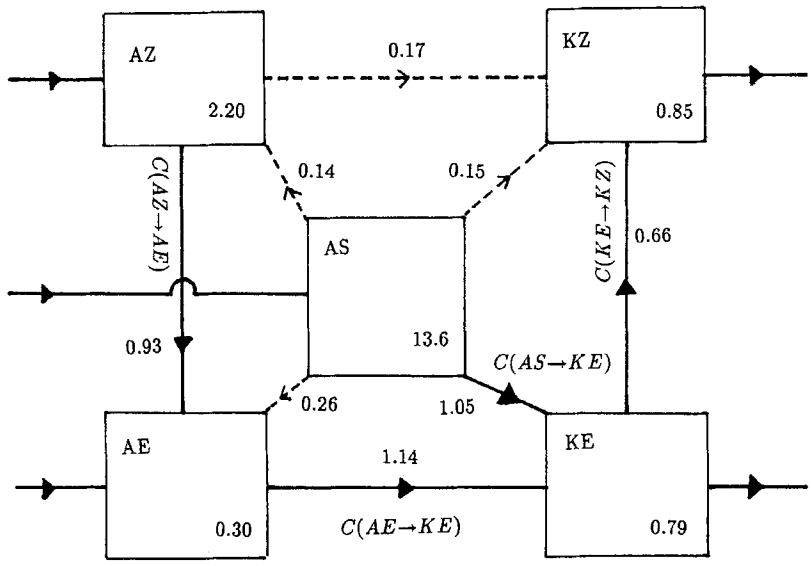

Figure 1. Global energy cycle of the atmosphere after Pearce (1978). AS—static stability available potential energy, AZ—zonal available potential energy, AE—eddy available potential energy, KZ—zonal kinetic energy and KE—eddy kinetic energy. Numbers refer to values obtained from a 19-level T42 analysis of ECMWF data for the DJF winter of 1990/91. All energies are in units of 10^6 J m^{-2} and all conversions are in units of W m^{-2}.

* Eddy in this paper refers to a deviation from the zonally symmetric state.

system. For a complete definition of the terms and a detailed description refer to Blackburn (1983).

Table 1 shows the energy components for the strong and weak diffusion cases for T21 and T42 and also shows the analysed 1990/91 results for comparison. It is not clear how much interannual variability there is in the energy cycle but in the absence of a longer climatology we shall take the 1990/91 analysis as a typical guide to the observations. With weakened diffusion, it can be seen that the zonal APE (AZ) decreases and the static stability APE (AS) increases; the eddy APE (AE) is relatively insensitive. AZ is related to the equator–pole temperature gradients and, as will be shown later, weakened diffusion results in weakened equator–pole temperature gradients in the troposphere. The kinetic energies in Table 1 behave differently at T21 and T42 resolution. At T21 resolution, weakened diffusion results in less KZ and more KE and brings the results more in agreement with the T42 results and the observations. At T42 resolution, the kinetic energies are relatively insensitive to changes in the diffusion. The T21 results are in agreement with the T31 ∇^4 results presented in Table 3 of Laursen and Eliasen (1989). The GCM results appear to have too much KZ and not enough KE compared to the observations. This may be related to the well known deficit of blocking events in atmospheric models that spend too much time in zonally symmetric states (Tibaldi 1992). The use of an energy-conserving scheme similar to APVM may help to alleviate this problem since APVM schemes have been shown to give more eddy kinetic energy than do conventional Laplacian schemes (Sadourny and Basdevant 1985).

Table 2 shows the major conversions of energy related to the baroclinic and barotropic processes. All the conversions show a weakening as the diffusion is decreased for both T21 and T42. The weakening of the baroclinic processes is consistent with the decrease in the equator–pole temperature gradient associated with diminished zonal available energy. The barotropic conversion C(KE → KZ) shows a strong dependence on the diffusion strength at both T21 and T42. At T21 resolution, weakened diffusion results in more KE and less barotropic conversion yet the systematic difference between T21 and T42 is that T21 has too little KE and too small a barotropic conversion. Hence, it appears that more than tuning the diffusion is necessary to make a T21 model emulate the global energy cycle of a T42 model; there can be more KE or more barotropic conversion but not both. Both the KE and the barotropic conversion response agree with

TABLE 1. GLOBAL ENERGIES IN UNITS OF 10^6 J m^{-2}

Model	AS	AZ	AE	KZ	KE
T21 4 h u4^6	13.0	2.60	0.26	1.11	0.40
T21 1 d ∇^{10}	13.6	2.16	0.27	0.98	0.53
T42 4 h ∇^6	13.3	2.54	0.27	1.02	0.56
T42 1 d ∇^{10}	13.6	2.37	0.27	1.01	0.56
DJF 1990/91	13.6	2.20	0.30	0.85	0.79

TABLE 2. MAJOR ENERGY CONVERSIONS IN UNITS OF W m^{-2}

Model	C(AZ → AE)	C(AE → KE)	C(AS → KE)	C(KE → KZ)
T21 4 h ∇^6	1.13	1.23	1.26	0.72
T21 1 d ∇^{10}	1.01	1.22	1.16	0.45
T42 4 h∇2^6	1.07	1.46	1.36	0.99
T42 1 d∇^{10}	0.94	1.31	1.20	0.81
DJF 1990/91	0.93	1.14	1.05	0.66

the lifecycle findings of MacVean (1983). The T42 baroclinic conversions to KE and the barotropic conversion from KE to KZ are all larger than the observations and this is consistent with the finding that higher resolution ECMWF forecast models have overly strong momentum flux convergences and subtropical jets which are too far poleward (World Meteorological Organization 1988; Boer and Lazare 1988; Boville 1991). The efficiency of the baroclinic eddies can be defined as the ratio of the conversion $C(AE \rightarrow KE)$ to the KE, in which case it can be seen that the efficiency decreases with weakened diffusion. The baroclinic eddies become less efficient when the equator–pole temperature gradient is weaker in accordance with the idea that the eddies try to adjust the temperature gradient back to the point of critical stability.

Tables 3 and 4 show the barotropic conversion and the kinetic energies in the (τ, q) parameter space for the T21 model. Monotonic trends with both τ and q can be seen indicating that both increased τ and increased q correspond to weaker diffusion. The barotropic conversion ranges greatly from 0.72 down to 0.15 W m^{-2} as the diffusion is weakened, and it is interesting to note that the sum of KE and KZ is relatively insensitive to the choice of diffusion.

(*b*) *The zonal-mean response*

The previous section demonstrated that, for both T21 and T42, there was a large global energy response to changes in the horizontal diffusion parametrization. The purpose of this section is to examine the response in more detail by analysis of zonal-mean quantities.

Figure 2 shows the zonal-mean zonal wind response to weakened diffusion for both the T21 and the T42 resolutions superimposed upon the 5 m s^{-1} contours of the time-averaged wind for the strong diffusion case. At both resolutions, there is an equivalent-barotropic weakening of the westerlies centred on 50°N and on 60°S; the poleward flanks of the jets weaken by about 10 m s^{-1} at T21 and by 5 m s^{-1} at T42. In addition, there is an equivalent-barotropic increase centred on 30°N having the net effect of strengthening the cyclonic barotropic shear between 30°N and 50°N on the poleward flank of the northern hemisphere subtropical jet. The response in the tropics shows no agreement between T21 and T42 resolutions and is the subject of further research. At T42, the southern hemisphere westerlies show a marked double-jet structure which is not seen at

TABLE 3. CONVERSION OF KE TO KZ IN UNITS OF W m^{-2} FOR THE T21 MODEL

$C(KE \rightarrow KZ)$	4 h	1 d	6 d
∇^{10}	0.65	0.45	0.15
∇^{8}	0.72	0.47	0.22
∇^{6}	0.72	0.53	0.23

TABLE 4. KINETIC ENERGIES (KZ, KE) IN UNITS OF 10^6 J m^{-2} FOR THE T21 MODEL

	4 h		1 d		6 d	
Kinetic energy	KZ	KE	KZ	KE	KZ	KE
∇^{10}	1.04	0.52	0.98	0.53	0.86	0.58
∇^{8}	1.07	0.49	1.02	0.53	0.87	0.58
∇^{6}	1.11	0.40	1.04	0.50	0.90	0.56

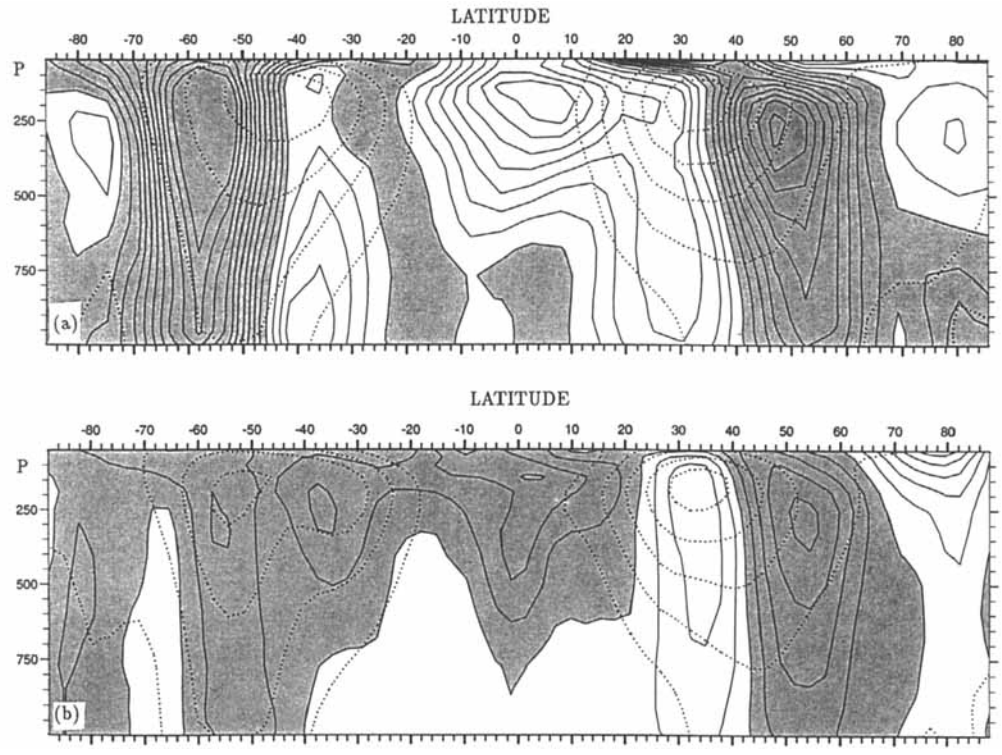

Figure 2. Zonal-mean zonal wind response 1 d ∇^{10}–4 h ∇^6 in units of 1 m s^{-1} with negative values shaded. (a) T21 response and (b) T42 response. Westerly dotted contours spaced every 10 m s^{-1} for the 4 h ∇^6 case are overlayed in order to demark the positions of the subtropical jets.

T21 and is a possible cause for the southern hemisphere difference in response between the two resolutions. The double-jet structure seen at T42 is less evident in the zonal-mean zonal wind observations and represents a systematic error of the model (Boer *et al.* 1992).

Figure 3 shows the zonal-mean temperature response which clearly demonstrates warming in the higher latitude troposphere as the diffusion is weakened with some associated cooling above the tropopause. This is in agreement with the findings from the global energy analysis, which showed a decrease in the zonal available energy. Weakening the diffusion causes a clear decrease in the tropospheric equator–pole temperature gradients which is consistent with the observed reduction in the baroclinic energy conversions.

Figure 4 shows the mean meridional mass circulation response superimposed on shading indicating the position of the strong diffusion Hadley, Ferrel and polar cells. The time-mean mean meridional mass circulation for the case of strong diffusion is presented in Fig. 2(a) of Slingo *et al.* (1994). For both resolutions, northern and southern Ferrel cells show a marked decrease in intensity implying less net heat transport to lower latitudes and hence more net heat transport to higher latitudes consistent with the high latitude warming previously discussed. At T42 resolution with strong diffusion, the northern hemisphere Ferrel cell transports roughly 4×10^{10} kg s^{-1} and shows a difference between 1 d ∇^{10} and 4 h ∇^6 diffusions of roughly 1.5×10^{10} kg s^{-1}. There seems to be little agreement in the tropical response at the different resolutions but it should be noted that the fractional change in the Hadley cells is much less than that in the Ferrel cells.

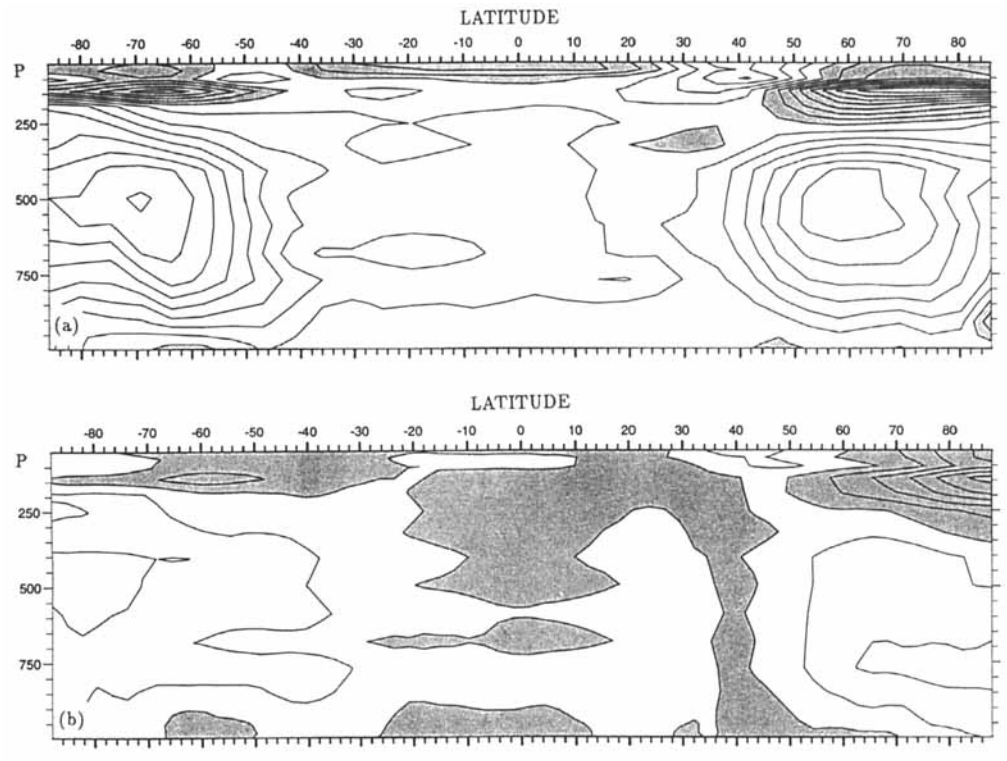

Figure 3. Zonal-mean temperature response 1 d ∇^{10}–4 h ∇^6 in units of 1 K with negative values shaded. (a) T21 response and (b) T42 response.

To a good approximation at upper-level mid latitudes, the time-mean meridional circulation is balanced by the convergence of poleward eddy momentum flux as can be seen from the time-mean zonal-mean of the zonal wind equation:

$$f\overline{[v]} = \frac{1}{a\cos^2\theta}\frac{\partial}{\partial\theta}(\cos^2\theta\overline{[u^*v^*]}).$$

Hence, a weakening of the Ferrel cells is expected to be linked to a weakening of the poleward eddy momentum flux convergence and changes in the upper-level poleward eddy momentum flux. Figure 5 shows the changes in the poleward eddy momentum flux, $[u^*v^*]$, which are appreciable compared to the typical climatological values of roughly 50–100 $m^2\,s^{-2}$. The changes are localized at upper levels and are centred upon 45°N and 50°S and correspond to the barotropic phase tilt of the eddies becoming less on the poleward sides of the jets when the diffusion is weakened. This effect, and the weakening of the westerlies on the poleward side of the jets, is the reason why the barotropic conversion of eddy to zonal kinetic energy is so sensitive to the diffusion scheme.

Figure 6 shows the response of the poleward transient momentum flux, $[u'v']$, and differs from the eddy momentum flux in Fig. 5 by not including the changes in the stationary eddies, $[\overline{u}^*\overline{v}^*]$, and by including the effect of zonal-mean transients, $[u'][v']$. In general, the zonal-mean transient fluxes are negligible compared to those of the eddies and hence the difference between Fig. 6 and Fig. 5 shows the response of the poleward momentum flux by the stationary eddies. It can be seen that a large part of the momentum flux change is due to changes in the transient eddies with the biggest exception

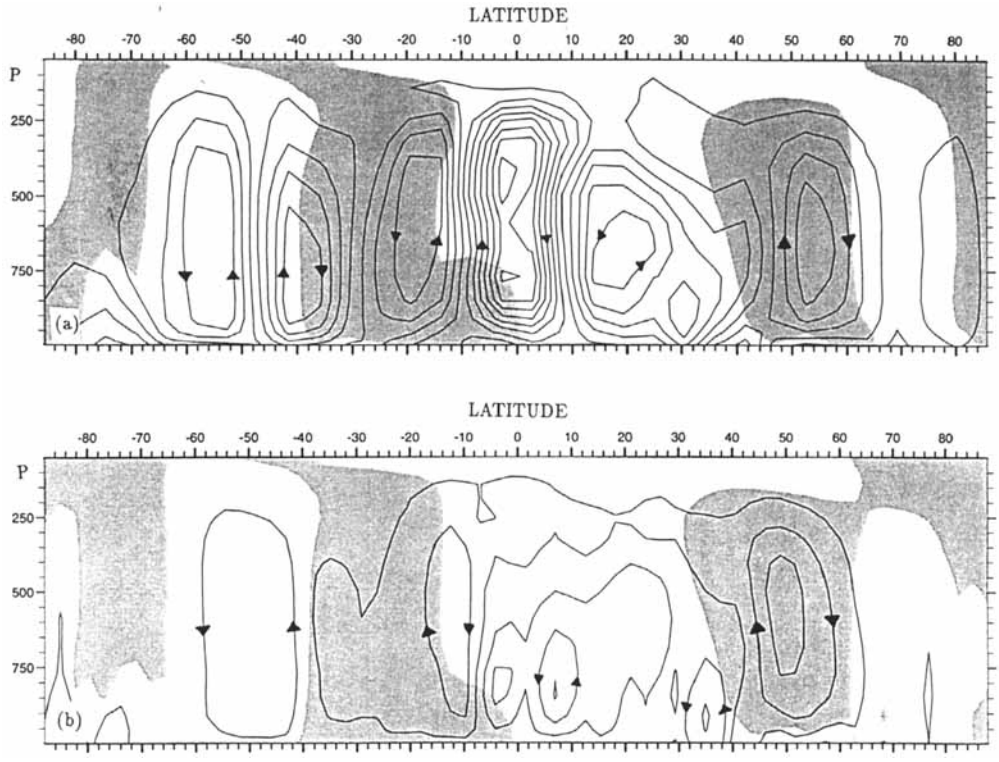

Figure 4. Mean meridional mass circulation response $1\,\mathrm{d}\,\nabla^{10}-4\,\mathrm{h}\,\nabla^{6}$ in units of $0.5 \times 10^{10}\,\mathrm{kg\,s^{-1}}$. Shading denotes regions of negative mean meridional mass circulation in the $4\,\mathrm{h}\,\nabla^{6}$ climatology in order to mark the position of the Hadley and Ferrel cells. (a) T21 response and (b) T42 response.

to this occurring in the northern hemisphere T21 response where a large change takes place in the stationary eddy flux.

Following Edmon *et al.* (1980), Eliassen–Palm (EP) diagnostics are shown in Fig. 7 in order to explain how the change in eddy fluxes forces the zonal-mean flow. Rather than show the full divergence of the EP flux, including the vertical divergence of the heat flux, only the horizontal divergence of the horizontal component of the EP flux is presented and shows the convergence of the poleward eddy momentum flux. As explained by Pfeffer (1987), this has the virtue of providing a clearer explanation of zonal-mean wind tendencies rather than by using the total EP divergence. The total EP divergence has a large part due to the vertical divergence of the vertical component, which is largely cancelled by the residual circulation, leaving the total zonal wind tendency as a small residual. Furthermore, the vertical divergence is strongly dependent on the static stability and becomes problematic when zonal means are taken near the ground.

Figure 7(a) shows the horizontal EP divergence and the EP vectors for the T42 climatology and demonstrates that the climatological effect of the mid-latitude eddies is to cause an upper-level momentum flux convergence at around 50°N and 55°S which in turn causes an acceleration of the zonal-mean zonal wind at these latitudes and drives the indirect Ferrel circulations (Pfeffer 1987). Figure 7(b) shows the T42 response to weakened diffusion, where it can be seen that there is less upper-level equatorward propagation of wave energy thereby giving a reduction in the flux convergence at 50°N and 55°S. The decrease in acceleration due to decreased flux convergence, explains why

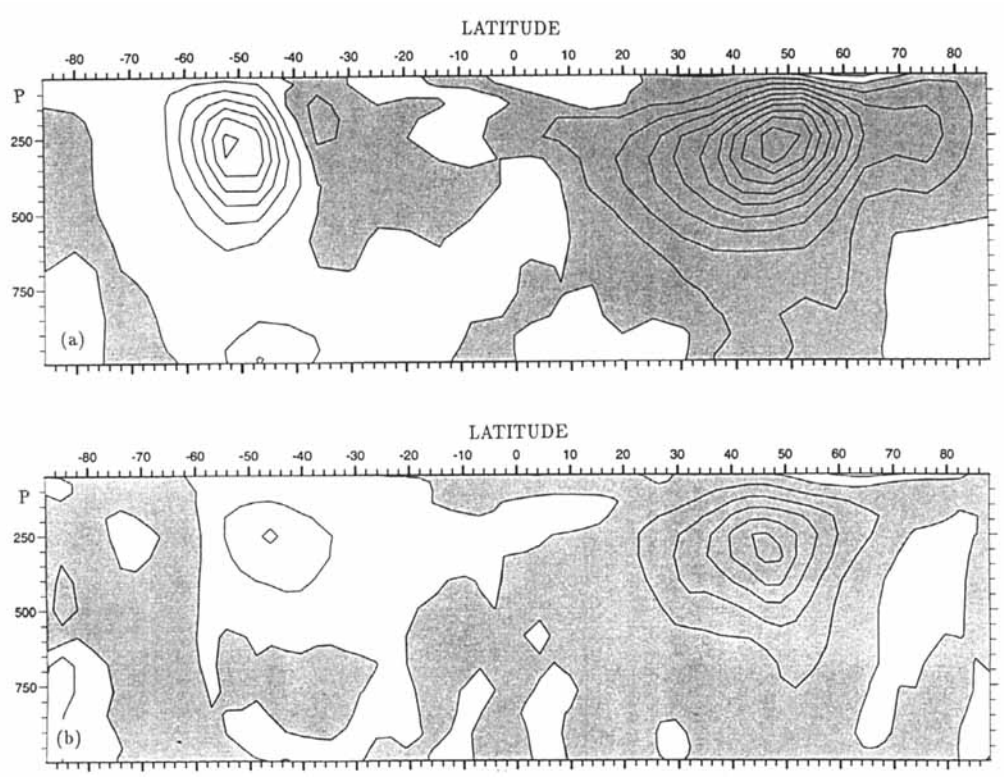

Figure 5. Zonal-mean poleward eddy momentum flux, $\overline{[u^*v^*]}$, response $1\,\mathrm{d}\,\nabla^{10}$–$4\,\mathrm{h}\,\nabla^{6}$ in units of $5\,\mathrm{m}^2\,\mathrm{s}^{-2}$ with negative values shaded. (a) T21 response and (b) T42 response.

both the Ferrel cells and the poleward flanks of the westerly jets weaken. The T21 results gave the same pattern of response as the T42 response but with about twice the amplitude, and for the sake of brevity we preferred to present just the T42 results which are more appropriate to current high resolution GCM experiments.

The northern hemisphere tropospheric response to weakened diffusion is similar to that obtained by strengthening the upper-level orographic gravity wave drag in that the poleward flank of the mid latitude jet weakens, the Ferrel cell weakens and the upper-level poleward eddy momentum flux convergence decreases (Stephenson 1993). A similar effect has been noted with the GCM at the Max Planck Institute in Hamburg (E. Manzini, personal communication). Speculating on the origin of the common response, it is of interest to note that one effect of including orographic gravity wave drag, as with weakening the horizontal diffusion, is to produce more transient small-scale features in the upper-level isentropic potential vorticity, which may then be reducing the transient eddy momentum fluxes by making the synoptic-scale baroclinic waves less coherent. Orsolini *et al.* (1993) have previously noted that the small-scale noise introduced by the gravity wave drag scheme is capable of decorrelating such quantities as the isentropic potential vorticity and the isentropic ozone mixing ratio in the lower stratosphere.

(*c*) *The eddy response*

The previous section explained the global energy cycle results by examination of zonal-mean diagnostics and found a response related to large changes in the convergence of the poleward momentum flux of the transient eddies. In this section, a brief examination

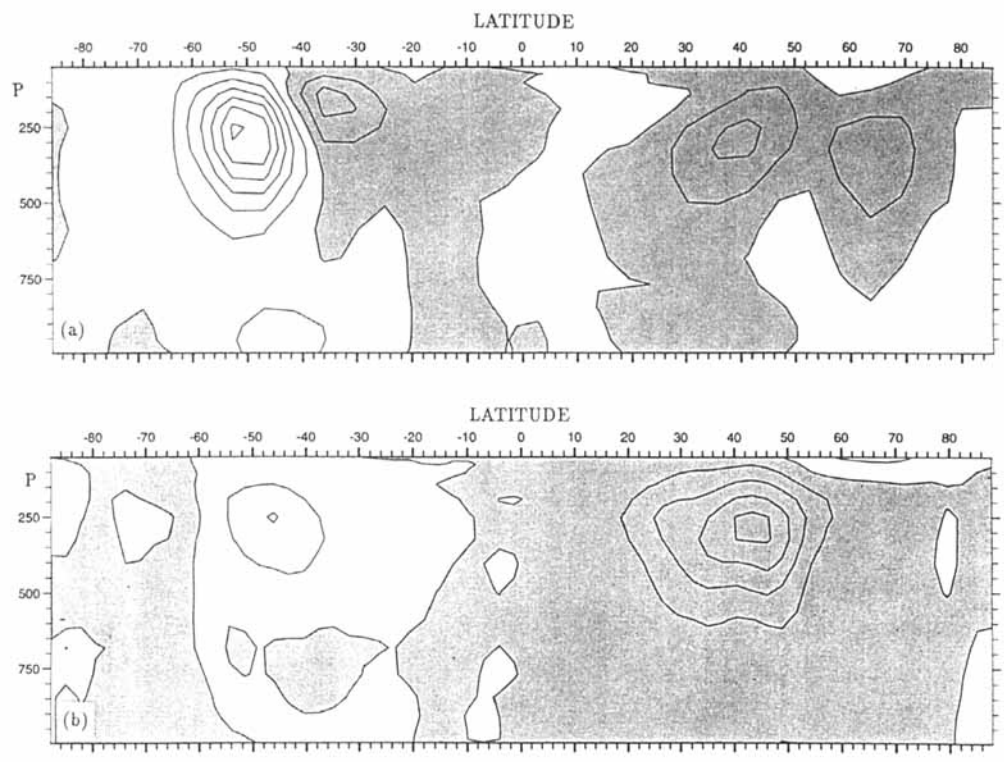

Figure 6. Zonal-mean transient poleward momentum flux, $\overline{[u'v']}$, response 1 d ∇^{10}–4 h ∇^6 in units of 5 $m^2 s^{-2}$ with negative values shaded. (a) T21 response and (b) T42 response.

will be made of the spatial distribution of the eddy response in the northern hemisphere. Only T42 results are shown as similar results were found at T21 resolution.

Figure 8 shows the climatology and the response of the three-day high-pass filtered transient poleward momentum flux at 250 mb in the T42 results; refer to Hoskins *et al.* (1989) for a description of the filter. In the climatology, regions of strong meridional gradient occur at the eastern end of the Pacific stormtrack and at the western end of the Atlantic stormtrack causing forcing of the zonal wind in these regions. The response to weakened diffusion is large and centred just to the south of these regions. The effect of weakened diffusion is to cause the region of negative $\overline{u'v'}$ correlation to extend further south and have a weaker meridional gradient.

Figure 9(a) shows the eddy part of the 250 mb streamfunction response to weakened diffusion. The magnitude is about a third of the climatological mean stationary wave amplitude. A wavetrain can be discerned heading from west of Alaska southwards to the tropical Atlantic in accordance with results from a linear barotropic model (T. Ambrizzi, personal communication). Figure 9(b) shows the eddy part of the 250 mb streamfunction response obtained by changing the weak 1989 ECMWF gravity wave drag scheme to the stronger 1986 gravity wave drag scheme in the UGAMP GCM (refer to Stephenson (1993) for more details). The response of the North American and Atlantic sectors shows a similar pattern of response to that with weakened diffusion in agreement with the previous statements that reduced diffusion acts in a similar way to strengthened orographic gravity wave drag.

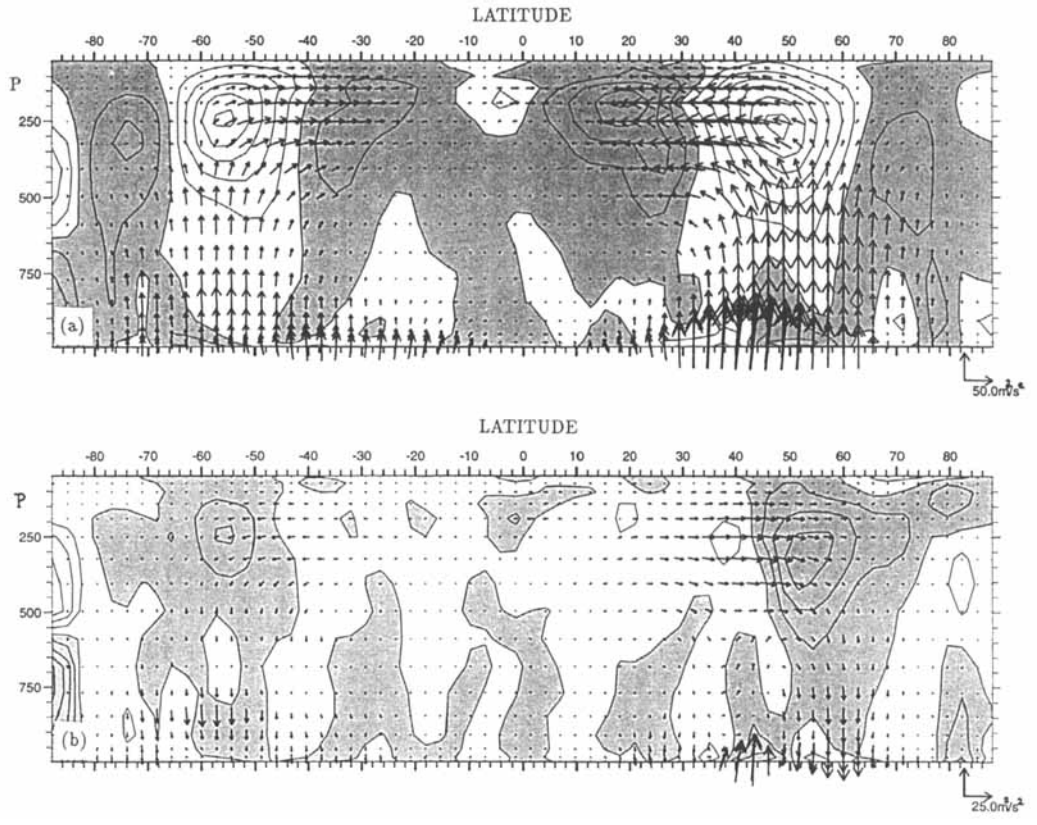

Figure 7. EP flux vectors superimposed on the horizontal divergence of the horizontal component of the EP flux with negative values shaded for (a) the 4 h ∇^6 T42 climatology in units of 1 m s^{-1} day^{-1} and (b) the 1 d ∇^{10}–4 h ∇^6 response in units of 0.5 m s^{-1} day^{-1}.

4. Discussion

This study has shown that moderate changes in the horizontal diffusion strength can have sizeable impacts on the simulation of the wintertime general circulation even at moderately high T42 resolution. It has been shown that it is impossible to tune the diffusion at T21 resolution to give a good representation of the global energy cycle and it remains an open and interesting question as to the sensitivity of high resolution GCMs (e.g. T106) to changes in the diffusion parametrization. Weakened diffusion results in weakened equator–pole temperature gradients, weakened baroclinicity and much weaker barotropic energy conversions. The transient eddy poleward momentum flux is especially sensitive. The weakened convergence of upper-level poleward eddy momentum flux results in weakened westerlies on the poleward flanks of the subtropical jets and weaker Ferrel cells consistent with EP diagnostics. A large upper-level stationary wave response is forced which appears to propagate from western North America into the tropical Atlantic. For all the fields examined, the northern hemisphere tropospheric response is similar to that seen when orographic gravity wave drag is strengthened at upper levels.

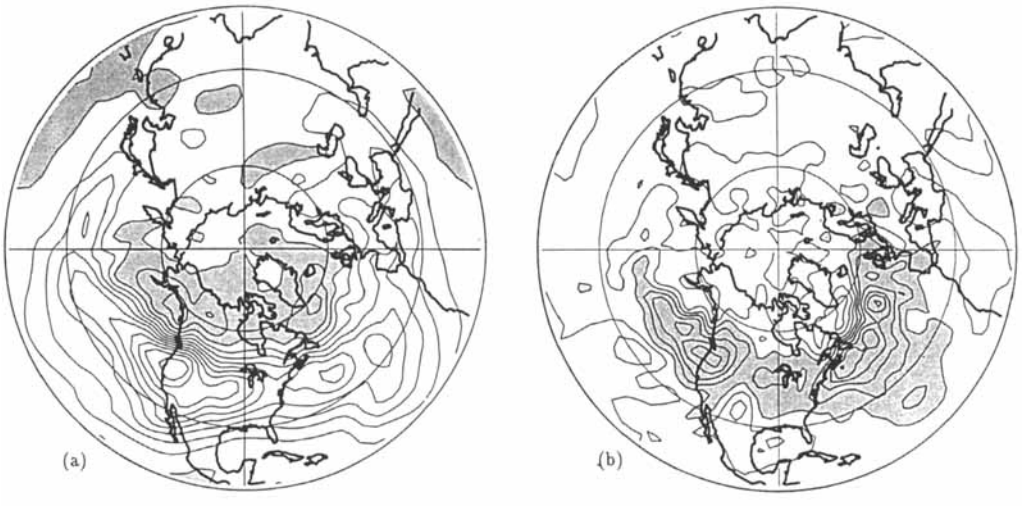

Figure 8. Transient high-passed $\overline{[u'v']}$ flux at 200 mb in units of $10\,m^2\,s^{-2}$ for (a) the $4\,h\,\nabla^6$ T42 climatology (negative values shaded) and (b) the $1\,d\,\nabla^{10}$–$4\,h\,\nabla^6$ response (values less than $-10\,m^2\,s^{-2}$ shaded).

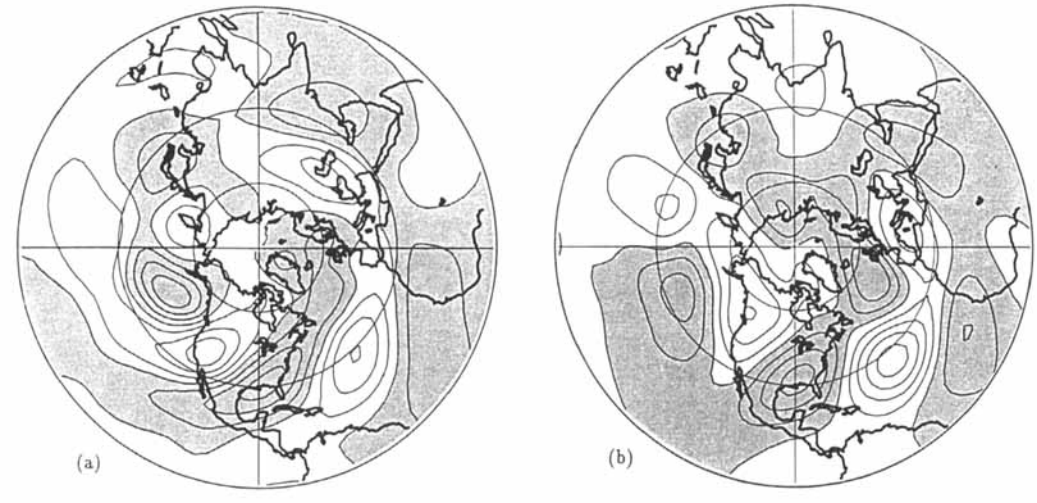

Figure 9. The eddy part of the 200 mb streamfunction with negative values shaded for (a) the $1\,d\,\nabla^{10}$–$4\,h\,\nabla^6$ response in units of $2.5 \times 10^6\,m^2\,s^{-1}$ and (b) the strong (1986) minus the weak (1989) ECMWF gravity wave drag scheme response in units of $5 \times 10^6\,m^2\,s^{-1}$.

The sensitivity of the GCM wintertime climatology to changes in the horizontal diffusion parameters shows that care should be taken when tuning these parameters. This is especially the case for studies of the effect of the horizontal resolution on the general circulation. Previous studies have relied on tuning the diffusion scheme by insisting upon the existence of an inertial range in the energy spectrum (Boer and Lazare 1988; Boville 1991). The small range of scales and the possible inability of the current horizontal diffusion schemes to reproduce accurately all the effects of sub-grid mixing, cause one to question such methods of tuning. It is possible that the non-convergence of

the eddy momentum flux, in the resolution experiments of Boville (1991), is an artefact of tuning the horizontal diffusion to be too strong at the higher resolutions by insisting that the energy spectrum in finite resolution models should have an inertial range.

This study has not addressed the dynamical problem of why the transient eddy poleward momentum fluxes are so sensitive to the strength of the horizontal diffusion. One possible mechanism is that described by Thorncroft *et al.* (1993). Two radically different types of baroclinic lifecycle were obtained, known as LC1 and LC2, depending upon the barotropic shear of the basic zonal-mean wind state. With stronger westerlies on the poleward edge of the subtropical jet (i.e. less cyclonic barotropic shear), the *basic* lifecycle, LC1, was obtained having backward-tilting, thinning troughs being advected anticyclonically and equatorward causing large wave-absorption and strong EP flux divergences. With weaker westerlies on the poleward edge of the subtropical jet, the *anomalous* lifecycle, LC2, was obtained characterized by forward-tilting, broadening troughs wrapping themselves up cyclonically to produce major cut-off cyclones in high latitudes with more wave reflection and smaller EP flux divergences. It is plausible that weaker diffusion favours LC2 type behaviour, with its stronger shear zones, and proposed future work plans to test this idea by developing objective measures of LC1 and LC2 behaviour.

ACKNOWLEDGEMENTS

This work would not have been possible without the kind help of the people at Reading University who maintain and develop the UGAMP GCM and especially Dr Mike Blackburn for his help with the global energetics analysis.

REFERENCES

Alexander, R. C. and Mobley, R. L. 1976 Monthly average sea-surface temperatures and ice-pack limits on a 1° global grid. *Mon. Weather Rev.*, **104,** 143–148

Blackburn, M. 1983 An energetics analysis of the general atmospheric circulation. University of Reading, U.K., PhD thesis

Boer, G. J., McFarlane, N. A., Laprise, R., Henderson, J. D. and Blanchet, J.-P. 1984 The Canadian Climate Centre spectral atmospheric general circulation model. *Atmos.-Ocean*, **22,** 397–429

Boer, G. J. and Lazare, M. 1988 Some results concerning the effect of horizontal resolution and gravity-wave drag on simulated climate. *J. Climate*, **1,** 789–806

Boer, G. J., Arpe, K., Blackburn, M., Déqué, M., Gates, W. L., Hart, T. L., le Treut, H., Roeckner, E., Sheinin, D. A., Simmonds, I., Smith, R. N. B., Tokioka, T., Wetherald, R. T. and Williamson, D. 1991 An intercomparison of the climates simulated by 14 atmospheric GCMs. WCRP Rep. 58, WMO/TD-425, World Meteorol. Organisation, Geneva

1992 Some results from an intercomparison of the climates simulated by 14 atmospheric general circulation models. *J. Geophys. Res.*, **97,** D12, 12771–12786

Bourke, W. 1974 A multi-level spectral model. I. Formulation and hemispheric integrations. *Mon. Weather Rev.* **102,** 687–701

Boville, B. A. 1991 Sensitivity of a simulated climate to model resolution. *J. Climate*, **4,** 469–485

Edmon, H. J., Hoskins, B. J. and McIntyre, M. E. 1980 Eliassen-Palm cross sections for the troposphere. *J. Atmos. Sci.*, **37,** 2600–2616

Eliasen, E. and Laursen, L. 1990 The effects of horizontal resolution and diffusion in a two-layer general circulation model with a zonally symmetric forcing. *Tellus*, **42A,** 520–530

Held, I. M., Lyons, S. W. and Nigam, S. 1989 Transients and the extratropical response to El Niño. *J. Atmos. Sci.*, **46**, 163–174

Held, I. M. and Phillips, P. 1993 Sensitivity of the eddy momentum flux to meridional resolution in atmospheric GCMs. *J. Climate*, **6**, 499–507

Hoskins, B. J., Hsu, H. H., James, I. N., Masutani, M., Sardeshmukh, P. D. and White, G. H. 1989 Diagnostics of the global atmospheric circulation. WCRP-27, WMO/TD-No. 326

Klinker, E. and Sardeshmukh, P. D. 1992 The diagnosis of mechanical dissipation in the atmosphere from large-scale balance requirements. *J. Atmos. Sci.*, **49**, 608–627

Laursen, L. and Eliasen, E. 1989 On the effects of the damping mechanisms in an atmospheric general circulation model. *Tellus*, **41A**, 385–400

Lorenz, E. N. 1955 Available potential energy and the maintenance of the general circulation. *Tellus*, **7**, 157–167

MacVean, M. K. 1983 The effects of horizontal diffusion on baroclinic development in a spectral model. *Q. J. R. Meteorol. Soc.*, **109**, 771–783

Morcrette, J.-J. 1990 Impact of changes to the radiation transfer parametrizations plus cloud optical properties in the ECMWF model. *Mon. Weather Rev.*, **118**, 847–873

Orsolini, Y., Cariolle, D. and Déqué, M. 1993 Ridge formation in the lower stratosphere and its influence on ozone transport: a GCM study during late January 1992. Submitted to *J. Geophys. Res.*, August 1993

Palmer, T. N., Branković, C., Molteni, F. and Tibaldi, S. 1990 Extended range predictions with ECMWF models: Interannual variability in operational model integrations. *Q. J. R. Meteorol. Soc.*, **116**, 799–834

Pearce, R. P. 1978 On the concept of available potential energy. *Q. J. R. Meteorol. Soc.*, **104**, 737–755

Pierrehumbert, R. 1991 Chaotic mixing of tracer and vorticity by modulated travelling Rossby waves. *Geophys. Astrophys. Fluid Dyn.*, **58**, 285–319

Pfeffer, R. L. 1987 Comparison of conventional and transformed Eulerian diagnostics in the troposphere. *Q. J. R. Meteorol. Soc.*, **113**, 237–254

Sadourny, R. and Basdevant, C. 1985 Parameterisation of subgrid scale barotropic and baroclinic eddies in quasi-geostrophic models: anticipated potential vorticity method. *J. Atmos. Sci.*, **42**, 1353–1363

Slingo, J., Blackburn, M., Betts, A., Brugge, R., Hoskins, B., Miller, M., Steenman-Clark, L. and Thuburn, J. 1994 Mean climate and transience in the tropics of the UGAMP GCM. Part 1: Sensitivity to convective parametrization. *Q. J. R. Meteorol. Soc.*, **120**, 881–922

Smagorinsky, J. 1963 General circulation experiments with the primitive equations: I. The basic experiment. *Mon. Weather Rev.*, **91**, 99–164

Stephenson, D. B. and Held, I. M. 1993 GCM response of northern winter stationary waves and storm-tracks to increasing amounts of carbon dioxide. *J. Climate*, **6**, 1859–1870

Stephenson, D. B. 1994 The northern hemisphere tropospheric response to changes in the gravity wave drag scheme in a perpetual January GCM. *Q. J. R. Meteorol. Soc.*, **120**, 699–712

Thorncroft, C. D., Hoskins, B. J. and McIntyre, M. E. 1993 Two paradigms of baroclinic-wave life cycle behaviour. *Q. J. R. Meteorol. Soc.*, **119**, 17–55

Tibaldi, S. 1992 Low frequency variability and blocking as diagnostic tools for global climate models. In Proceedings of the NATO workshop on the *Prediction of Interannual Climate Variations*. Ed. J. Shukla. Trieste 22–26 July 1991

Tiedtke, M., Heckley, W. A. and Slingo, J. 1988 Tropical forecasting at ECMWF: On the influences of physical parametrization on the mean structure of forecasts and analyses. *Q. J. R. Meteorol. Soc.*, **114**, 639–664

World Meteorological Organization (WMO) 1988 Report on the CAS/JSC Workshop on systematic errors in models of the atmosphere. WMO/TD-273, Geneva